Chapter 38

Magnetic Resonance Imaging of Human Brain Function

Jens Frahm, Peter Fransson and Gunnar Krüger

Introduction

Noninvasive methods for studying metabolic and functional properties of the central nervous system provide new tools for understanding the human brain at the system level. As a bridging technology between basic neurobiologic research in (transgenic) animals, system-oriented studies in humans, and medical applications to patients with neurologic disease, magnetic resonance is expected to gain further importance in linking advances in molecular neurobiology and neurogenetics to cerebral metabolism and physiology and even beyond to human brain function.

MRI

Over the past two decades magnetic resonance imaging (MRI) has evolved into the premier modality for mapping structural anatomy at high spatial resolution and with exquisite soft tissue contrast (Stark and Bradley 1998). Parallel advances extended the range of evaluations to cellular metabolism by localized MR spectroscopy (cf. Chapter 40), adding a biochemical dimension to anatomic imaging (Bachelard 1997). Functional aspects became available through magnetic resonance angiography, perfusion studies, diffusion contrast, and magnetization transfer techniques. For neuroscientists, the most fascinating development is the discovery that suitable MRI techniques are able to map the functional anatomy of the human brain – visualizing the processes of thinking and feeling.

Neuroimaging

The use of MRI for functional neuroimaging is attractive because it
- is noninvasive,
- offers repeated studies of individual subjects and patients,
- provides access to submillimeter spatial resolution,
- yields an efficient temporal resolution of about 1s, and
- allows for flexibility in the design of cognitive paradigms.

Moreover, high-field clinical MRI units are much more widely distributed and less costly than positron emission tomography (PET) systems (cf. Chapter 39) as the major alternative for functional mapping apart from single photon emission computed tomography (SPECT) as well as electroencephalographic (EEG; cf. Chapter 35) and magnetoencephalographic (MEG; cf. Chapter 37) recordings.

Correspondence to: Jens Frahm, Biomedizinische NMR Forschungs GmbH, Max-Planck-Institut für biophysikalische Chemie, Göttingen, D-37070, Germany (phone: +49-551-201-1721; fax: +49-551-201-1307; e-mail: jfrahm@gwdg.de)
Peter Fransson, Karolinska Institutet, MR Research Center, Department of Clinical Neuroscience, Stockholm, Sweden
Gunnar Krüger, Stanford University, Department of Radiology, Palo Alto, CA, 94305, USA

Oxygenation

Experimental work in animals first demonstrated that the level of cerebral blood oxygenation influences the signal intensity of T2*-weighted gradient-echo MR images (Ogawa et al 1990, Turner et al 1991). Whereas oxyhemoglobin is diamagnetic, deoxygenated hemoglobin serves as an endogenous paramagnetic contrast agent that dephases the nuclear spins of water protons in its direct vicinity, i.e., primarily within the venous microvasculature and surrounding tissue.

Contrast

The physical effect is a signal loss in MR images which integrate pertinent magnetizations over an image pixel during the acquisition process. The degree of signal loss depends on the absolute concentration of deoxyhemoglobin per voxel and scales with voxel size and gradient-echo time, i.e., the differential precession of spin moments between excitation and detection. For example, if an increase in cerebral blood flow and oxygenation decreases the deoxyhemoglobin concentration, then both the effective spin-spin relaxation time T2* and the corresponding signal intensity of a gradient-echo image show a concomitant increase. This blood oxygenation level dependent (BOLD) contrast may be enhanced by acquiring the signal at prolonged echo times of, for example, 30 to 50 ms depending on field strength and MRI technique.

Function

The demonstration of oxygenation sensitivity in animal imaging was rapidly followed by the observation that BOLD contrast may be exploited for functional mapping of the human brain (Kwong et al 1992, Ogawa et al 1992, Bandettini et al 1992, Frahm et al 1992, Blamire et al 1992). The driving force is the observation that a change in neuronal activity – often termed activation – causes a rise in cerebral blood flow that at least transiently "uncouples" from oxygen consumption (Fox and Raichle 1986, Frahm et al 1996) and therefore results in a venous hyperoxygenation, i.e., decreased deoxyhemoglobin. Although the full details of the hemodynamic and metabolic correlates associated with brain activation are not yet fully understood, the corresponding MRI signal intensity rise after stimulus onset is easily detectable and well documented for visual, auditory, and sensorimotor cortical processing.

Mechanisms

Similar to neuroimaging by PET, MRI studies of brain function rely on `secondary signals' that link changes in neuronal activity to correlated alterations of

- metabolism (e.g., glucose and oxygen consumption),
- perfusion (blood flow and blood volume), and
- blood oxygenation (deoxyhemoglobin).

The mainstream of techniques focuses on perfusion-related changes of the intravascular concentration of paramagnetic deoxyhemoglobin. Figure 1 conceptionally sketches the transformation of a change in focal neuronal activity into an MRI-derived activation map. The scheme indicates putative interferences at several levels ranging from data acquisition and signal processing to physiologic mechanisms and details of the paradigm design.

Key Message

Thus, a key to understanding MR functional neuroimaging is the fact that it does not measure neuronal activity directly. An important question therefore is: how can we reliably detect a change in neuronal activity at the physiologic level? To answer this question we need to examine the neurovascular and neurometabolic coupling under various experimental and clinical conditions, e.g., with respect to confounding modulations caused by medication, brain disease, or even paradigm timings, and to carefully optimize the experimental strategies.

Outline

The purpose of this chapter is to review the mainstream of MRI techniques proposed for successfully mapping brain activation. It introduces into the methodology and raises

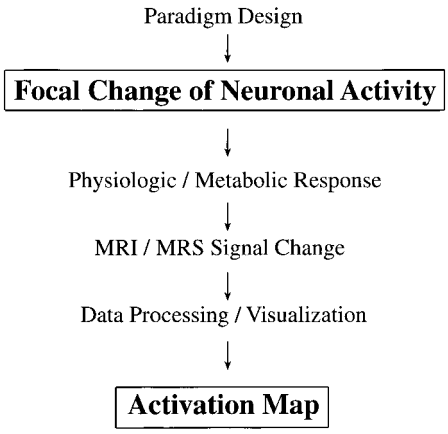

Fig. 1. Schematic diagram demonstrating the transformation of a focal change of neuronal activity into an activation map. MRI responses to brain activation (i) reflect differences in the experimental paradigm and its particular design, (ii) are sensitive to modulations of the neurovascular and/or neurometabolic coupling, and (iii) may be influenced by technical aspects of data acquisition and data processing including visualization and statistical treatment.

the awareness of potential pitfalls such as physiologic interferences. To accomplish these goals, the chapter will address

- technical aspects of MRI data acquisition,
- data analysis from dynamic MRI signals to activation maps
- physiologic aspects underlying MRI signals, and
- the design of suitable activation paradigms.

Technical Aspects of MRI Data Acquisition

Sequences for Brain Mapping

Principles

MRI comprises a large variety of radiofrequency (RF) and magnetic field gradient sequences for the acquisition of image data. Whereas RF pulses accomplish signal excitation, gradient pulses are required for a spatial discrimination of the excited MRI signals within a three-dimensional object.

In particular, RF excitation of a two-dimensional cross-section is based on the simultaneous application of an RF pulse and a slice selection gradient. Spatial information about the selected image section is encoded into the phase and frequency of its MRI signal by perpendicular gradients applied before and during signal acquisition. Image reconstruction is usually performed by two-dimensional Fourier transformation. Three-dimensional extensions are possible by adding an independent phase-encoding gradient along the direction of the slice selection gradient. Basic MRI principles, details of imaging sequences, and medical applications are summarized in Stark and Bradley (1998).

Fast Imaging

MRI sequences that are best suited for functional neuroimaging should be both fast and sensitive to changes in the deoxyhemoglobin concentration. These conditions are fulfilled for gradient-echo imaging techniques with prolonged echo times. Basic RF and gradient schemes for the most commonly used high-speed EPI (echo-planar imaging) and rapid FLASH (fast low angle shot) technique are shown in Figure2. The diagrams illustrate the aforementioned combinations of RF pulses and gradients for cross-sectional imaging.

EPI

The main characteristic of single-shot EPI is that the technique acquires all gradient echoes needed for image reconstruction after excitation by a single slice-selective RF pulse. The individual echoes are generated by multiply alternating the sign of the fre-

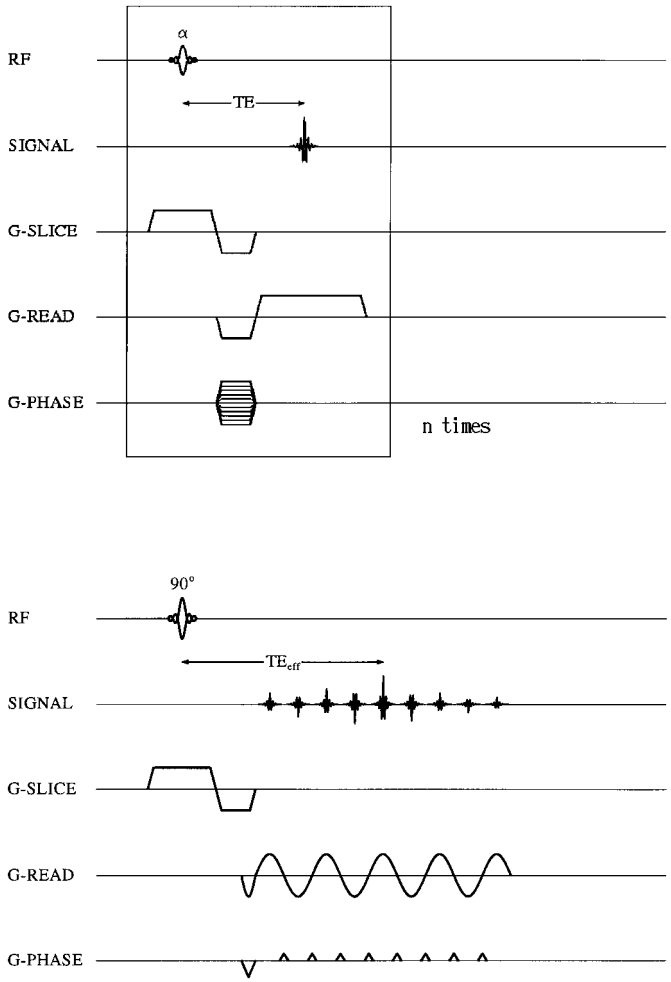

Fig. 2. Schematic radiofrequency (RF) and magnetic field gradient (G-SLICE, G-READ, G-PHASE) sequences for (top) FLASH (fast low angle shot) MRI and (bottom) single-shot gradient-echo EPI (echo-planar imaging) with blipped phase-encoding and symmetric coverage of *k* space. FLASH sequences employ multiple RF pulses with low flip angles $\alpha < 90°$ and generate only a single gradient echo (SIGNAL) per repetition interval by inversion of the frequency-encoding read gradient. EPI sequences acquire all differently phase-encoded gradient echoes after the application of a single RF excitation pulse.

quency-encoding "read" gradient (corresponding to 180° rotations of its direction). They represent individual lines of data points (Fourier lines) in the two-dimensional data space (*k* space). Phase encoding of shifted lines is accomplished by a "blipped" gradient between successive gradient echoes.

Data acquisition of EPI sequences is done during the decay of the excited MRI signal which is characterized by the effective spin-spin relaxation time T2*. The T2* sensitivity of the resulting image is determined by the gradient echo time TE, i.e., the period between RF excitation and signal acquisition. Because the individual echoes in EPI span a large range of different echo times, the effective TE value is given by the Fourier line representing the lowest spatial frequency. This Fourier line corresponds to the gradient echo with zero phase encoding and dominates the overall image contrast.

Typical imaging times are on the order of 100 ms, matrix sizes are usually 64 × 64 or 64 × 128 data points.

Spirals

An alternative high-speed MRI technique that may be used for functional neuroimaging is spiral scanning where coverage of the data space starts in the center and follows an outward spiral. Pertinent gradient schemes and image reconstruction schemes are slightly more complex than Fourier imaging of a rectangular grid of data points commonly employed for EPI and FLASH.

FLASH

The FLASH technique resembles a conventional MRI sequence in using multiple RF excitations and repetition intervals that each generate only one phase-encoded MRI signal.

In order to keep the overall imaging time short, the technique relies on a combination of RF pulse excitations with flip angles less than 90° and the acquisition of gradient echoes. Because the choice of a large TE value for obtaining sufficient T2* contrast directly prolongs the repetition period, typical imaging times are in the range of several seconds. The trade-off between temporal and spatial resolution is freely controllable via the number of phase-encoded gradient echoes, i.e., the number of repetition intervals.

The FLASH option is best exploited for mapping brain activation at high spatial resolution.

Image Contrast

Relaxation

The basic MRI contrast parameters are given by the proton spin density (e.g., water concentration), the proton T1 relaxation time denoting the exponential recovery of the longitudinal magnetization after excitation, and the proton T2 relaxation time describing the decay of the excited and detected transverse magnetization. In addition, gradient-echo signals such as those used in EPI and FLASH are subject to an even faster decay process phenomenologically characterized by the effective relaxation time T2*. It combines true T2 relaxation with the effects of magnetic field inhomogeneities including distortions that are caused by paramagnetic molecules such as deoxyhemoglobin.

Spin Density

In order to reduce the MRI sensitivity to signal fluctuations caused by vascular flow, brain tissue pulsations, and head motions, it is recommended to avoid T1 contrast when acquiring raw images for functional brain mapping. Instead, the images should be spin-density weighted in combination with T2* sensitivity, i.e., prolonged TE.

Spin density contrast is achieved under fully relaxed conditions using sufficiently long recovery periods before re-exciting the longitudinal magnetization, or by lowering the flip angle well below 90° for acquisitions with repetition times TR < 3 T1.

At 1.5–2.0 T field strength suitable combinations of TR and flip angle are 6000 ms/90°, 2000 ms/70°, 1000 ms/50°, 500 ms/30°, 200 ms/20°, 100 ms/15°, and 50 ms/10°. These parameters apply to both serial EPI and FLASH sequences.

Images

Examples of spin-density weighted EPI and FLASH images with T2* sensitivity are shown in Figure 3. For a fixed field-of-view of 200 mm the images illustrate the achievable image quality and contrast for pixel matrices of 64 × 64 and 128 × 128 (EPI and FLASH) as well as 256 × 256 (FLASH) in comparison to a flow-sensitized anatomic FLASH image of the same section.

Macroscopic Susceptibility Artifacts

The magnetic field pertubations induced by paramagnetic deoxyhemoglobin in and around the cerebral microvasculature are microscopic in nature (i.e., extending over distances of less than 50 μm) and well below the linear dimension of a typical image voxel (e.g., 1 mm).

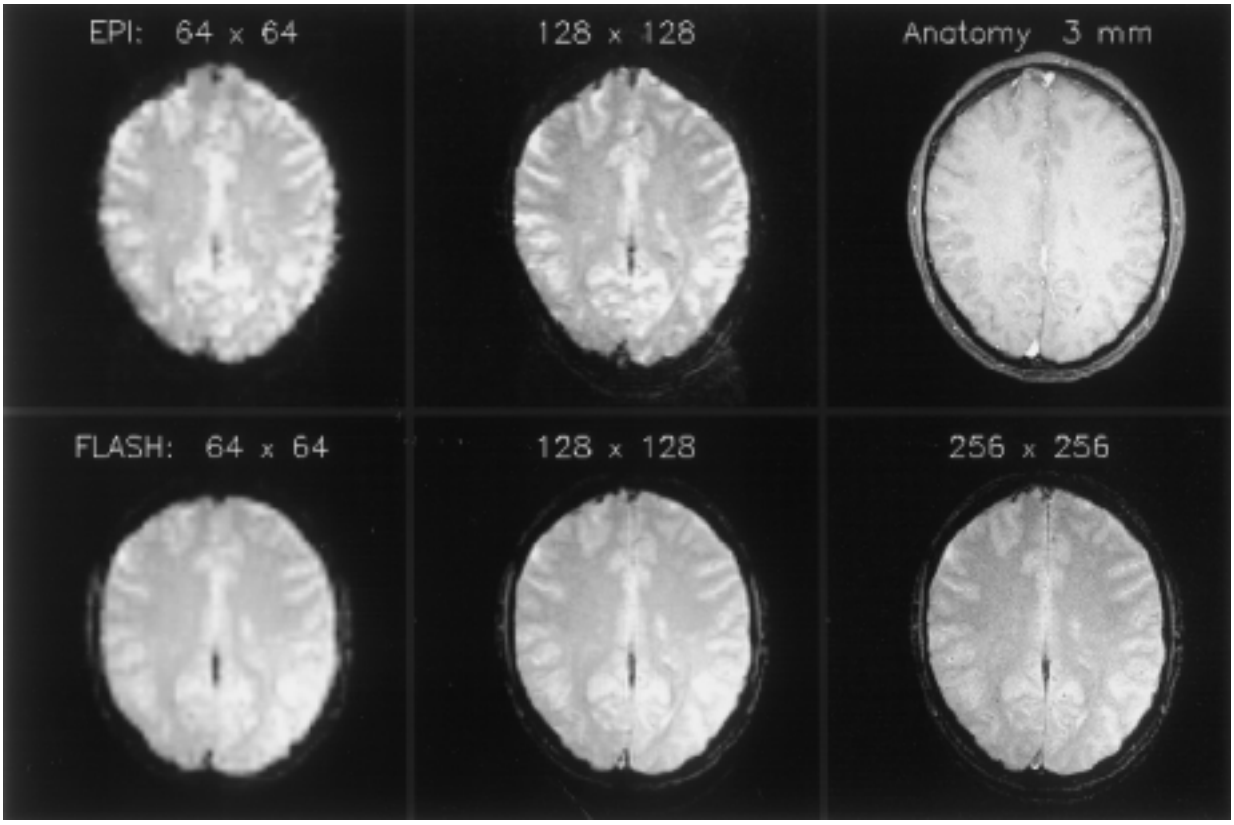

Fig. 3. Contrast and resolution of (top) EPI and (bottom) FLASH images commonly employed for functional neuroimaging (2.0 T, 200 mm field-of-view, 3 mm slice thickness) in comparison to a flow-sensitized T1-weighted FLASH image of the section anatomy (top right). Imaging parameters were adjusted such as to avoid T1 weighting and to ensure spin-density contrast (i.e., TR = 6000 ms and flip angle 90° for EPI as well as TR = 62.5 ms and flip angle 10° for FLASH) in combination with T2* sensitivity (i.e., an effective TE = 54 ms for EPI and TE = 30 ms for FLASH).

In addition, however, EPI and FLASH images with prolonged gradient echo times exhibit unwanted sensitivities to macroscopic magnetic field inhomogeneities from structural effects that usually extend over several voxels. They mainly originate from strong magnetic susceptibility differences at air-tissue interfaces, e.g., near the acoustic canals and the cavities at the cranial base. The resulting images are affected by signal loss and geometric distortions.

The brain section chosen for the images shown in Figure 3 suffers from only few macroscopic inhomogeneities. Nevertheless, the presence of small susceptibility differences, e.g., at the borderline of the frontal brain, leads to visible image degradation in the low-resolution 64 × 64 EPI image.

Signal Loss

Inhomogeneity problems become dramatic when moving to a section through the lower part of the brain as shown in Figure 4. The images clearly demonstrate that the sensitivity to macroscopic inhomogeneities poses a key problem for MR functional neuroimaging. For example, psychiatric interest in studying functional encoding in (anterior) hippocampal structures may be severely hampered by this problem.

Voxel Size

Susceptibility artifacts are less pronounced in FLASH images because of their conventional way of covering *k* space and their use of a fixed time for all gradient echoes. They

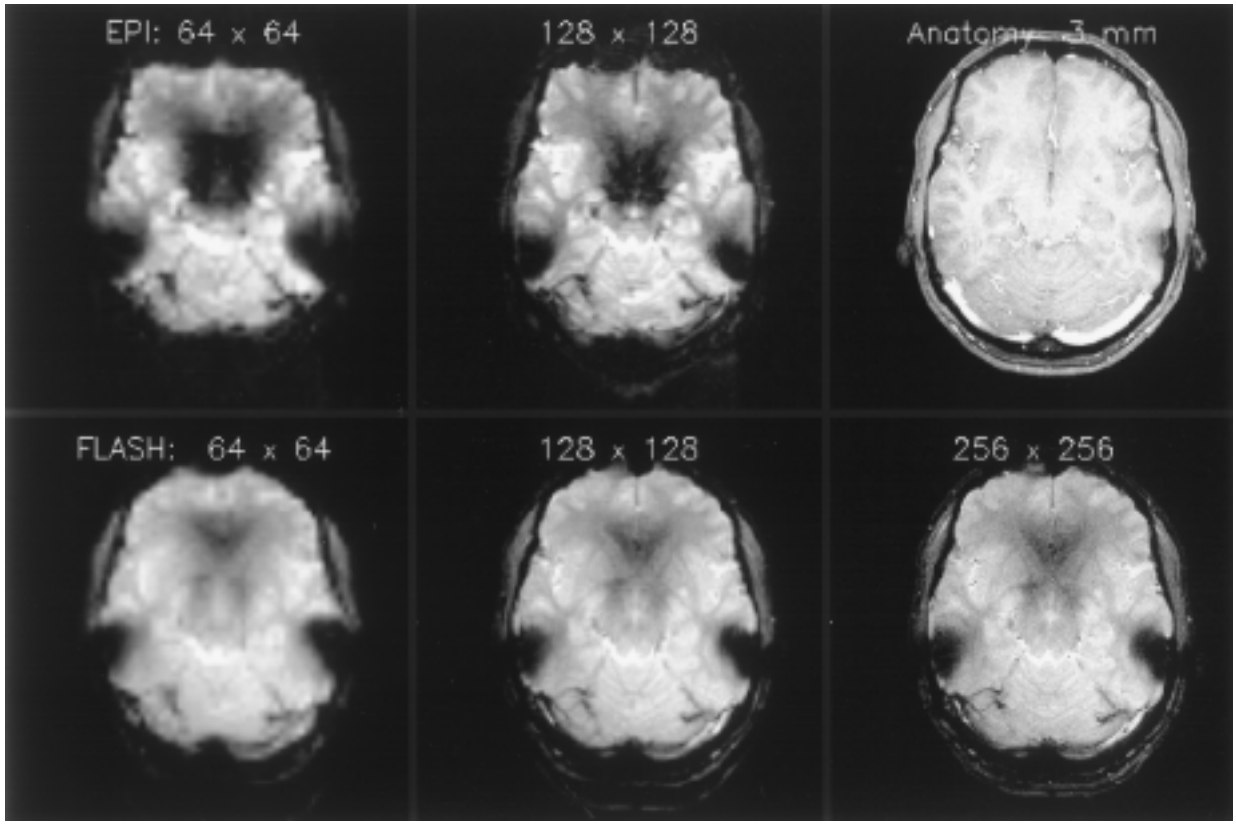

Fig. 4. Macroscopic susceptibility artifacts caused by air-tissue interfaces in (top) EPI and (bottom) FLASH images commonly employed for functional neuroimaging in comparison to a flow-sensitized anatomic FLASH image of the same section (top right). The data originate from the same subject as in Figure 3 using identical imaging parameters except for choosing a section through the lower part of the brain. The artifacts represent signal losses (EPI, FLASH) and geometric distortions (EPI) that increase with pixel size, i.e., reduced spatial resolution.

can be further reduced by using very small voxel sizes, i.e., very high spatial resolution and thin sections, which decrease the influence of macroscopic field gradients but retain the sensitivity to deoxyhemoglobin-induced intravoxel effects. These strategies are at the expense of temporal resolution and volume coverage.

Flow and Motion Sensitivity

Confounding signal fluctuations in serial MRI acquisitions may be induced by vascular flow, breathing, and involuntary subject movements. For both FLASH and EPI, it is therefore recommended to adjust flip angles and repetition times such as to avoid T1 weighting and thereby minimize the sensitivity of the steady-state longitudinal magnetization to amplitude fluctuations.

Intrascan phase effects such as ghosting may be minimized by optimized gradient waveforms and/or the use of navigator echoes. Moreover, the maximum imaging times should be kept to below 10 s to avoid complications from respiratory motions with time periods on the order of 5–6 s.

Head Motion

A most relevant interscan motion problem may result from stimulus-correlated head or body movements during the applied paradigm. For example, a typical observation is a

slight nodding movement of the subject's head as well as a continuous drift or rotation during an experiment of several minutes. Whereas the latter effects may be alleviated with the help of suitable post-acquisition motion correction algorithms, the former influence may even be difficult to detect unless major correlated motions lead to a spatially unspecific emphasis of all contrast borders in the resulting activation map.

Control

In general, it is recommended to control the MRI data quality by a rapid cine display of the serial images. Often it might be preferable to repeat an experiment rather than to rely on a proper correction of artifacts. Motion problems may become dramatic when studying patients instead of motivated healthy volunteers. In special cases it may be helpful to use fixation devices such as bite bars.

Temporal and Spatial Resolution

Depending on study purpose and the underlying scientific or clinical question, the necessary choice of a compromise between
- temporal resolution,
- volume coverage, and
- spatial (in-plane) resolution

should be based on single-shot EPI (spirals) or FLASH, respectively.

EPI

EPI emphasis is on high speed yielding imaging times on the order of 100 ms which translate into a maximum temporal resolution of 100 ms for single slice acquisitions. Alternatively, EPI offers excellent volume coverage by multi-slice imaging as up to 20 sections may be scanned with a repetition time of 2 s.

In general, the in-plane resolution of EPI sequences is limited because of the limited number of gradient echoes that can be acquired during the T2* signal decay after RF excitation. A typical in-plane resolution for EPI is 3×3 mm^2, but 2×2 mm^2 are possible. Slice thicknesses are generally 3–4 mm, but some groups still use 5–10 mm sections.

FLASH

FLASH applications are complementary to the more commonly used EPI technique. They facilitate access to high spatial resolution at the expense of temporal resolution and volume coverage. Attempts to maximize the in-plane resolution may even be limited to single sections.

Typically, FLASH images with a 96×256 data matrix, a rectangular field-of-view of 150×200 mm^2, and zero-filling by a factor of 2 during Fourier transformation result in an in-plane resolution of 0.78×0.78 mm^2 and a temporal resolution of a few seconds. Pertinent strategies may be further optimized to allow for high-resolution mapping of the columnar organization of the human cortex. Section thicknesses are 3–4 mm but may be reduced to 1 mm.

Magnetic Field Strength

1.5–3.0 T

The choice of the "optimum" magnetic field strength for MR functional neuroimaging is an unresolved issue. The results presented here are obtained at 2.0 T (Siemens Vision, Erlangen, Germany), while most clinical systems are likely to continue operating at 1.5 T (or below). More recently, a few dedicated head systems became available at 3.0 T.

T2* etc.

In general, the effects of magnetic field inhomogeneities and susceptibility differences – or in other words the 1/T2* relaxation rate – increase with field strength. Thus, be-

cause the T2* relaxation time becomes shorter, the useful length of the EPI data acquisition period is further reduced. On the other hand, the possibility of selecting shorter gradient echo times at higher fields may be an advantage for FLASH sequences. Other considerations refer to the fact that not only the signal-to-noise ratio but also the unwanted sensitivity to motion and macroscopic inhomogeneities increase with field strength.

Contrast

It is therefore not yet clarified whether – or under which circumstances – putative improvements in "functional contrast-to-noise" as the crucial criterion justify the investment of a 3.0 T system. In any case, it is recommended to rely on commercially available equipment, i.e., complete MRI systems from the leading manufacturers in diagnostic imaging.

Data Evaluation and Visualization

A Simple Experiment

Functional information about the human brain is extracted from serial MR images acquired over a period of several minutes. During this period the subject reacts in response to a paradigm that involves at least two different conditions, i.e., functional states exhibiting different degrees of neuronal activity.

Anatomy

Figure 5 summarizes some of the elements of a simple visual mapping experiment. It compares the neuronal representations of processing flickerlight and darkness in a single oblique MRI section along the calcarine fissure. Typically, the experiment starts with the acquisition of the individual 3D anatomy for retrospective referencing, the definition of the desired section(s), and a visualization of the local anatomy and (macro-) vasculature (top panels).

BOLD Images

These preparatory steps are followed by application of the paradigm with simultaneous dynamic acquisitions of the functional images. The middle panels of Figure 5 depict spin-density weighted FLASH images with T2* sensitivity at a temporal resolution of 6 s and a spatial resolution of 0.78×0.78 mm^2. Relative to images acquired during darkness (middle left) flickerlight stimulation (middle right) reveals a focal increase in MRI signal intensity, i.e., a decrease in deoxyhemoglobin, in selected areas of visual cortex. Visual stimulation was accomplished by a projection setup covering $40° \times 30°$ of the subject's visual field (Schäfter & Kirchhoff, Hamburg, Germany).

Raw Data

The direct experimental result is a series of consecutive images yielding MRI signal intensity time series for each image pixel. Using multi-slice acquisitions (e.g., 20 sections), high temporal resolution (e.g., 2 s), moderate spatial resolution (e.g., 128×128 data matrix), and a 5 min activation protocol, the raw data of a single experiment already amounts to 3000 images or 96 Mbyte. With a cooperative volunteer and a measuring time of 1.5 hours at least 10 successive experiments are possible yielding about 1 Gbyte per session. Thus, also data storage and on-line computational times of sequential experiments have to be accounted for in planning a study.

Difference Map

The desired result is a single "activation" map per section that transforms any paradigm-specific MRI signal change into a color-coded quantity. Pertinent pixel values are summarized in a map which is commonly overlayed onto an anatomic image or functional raw image.

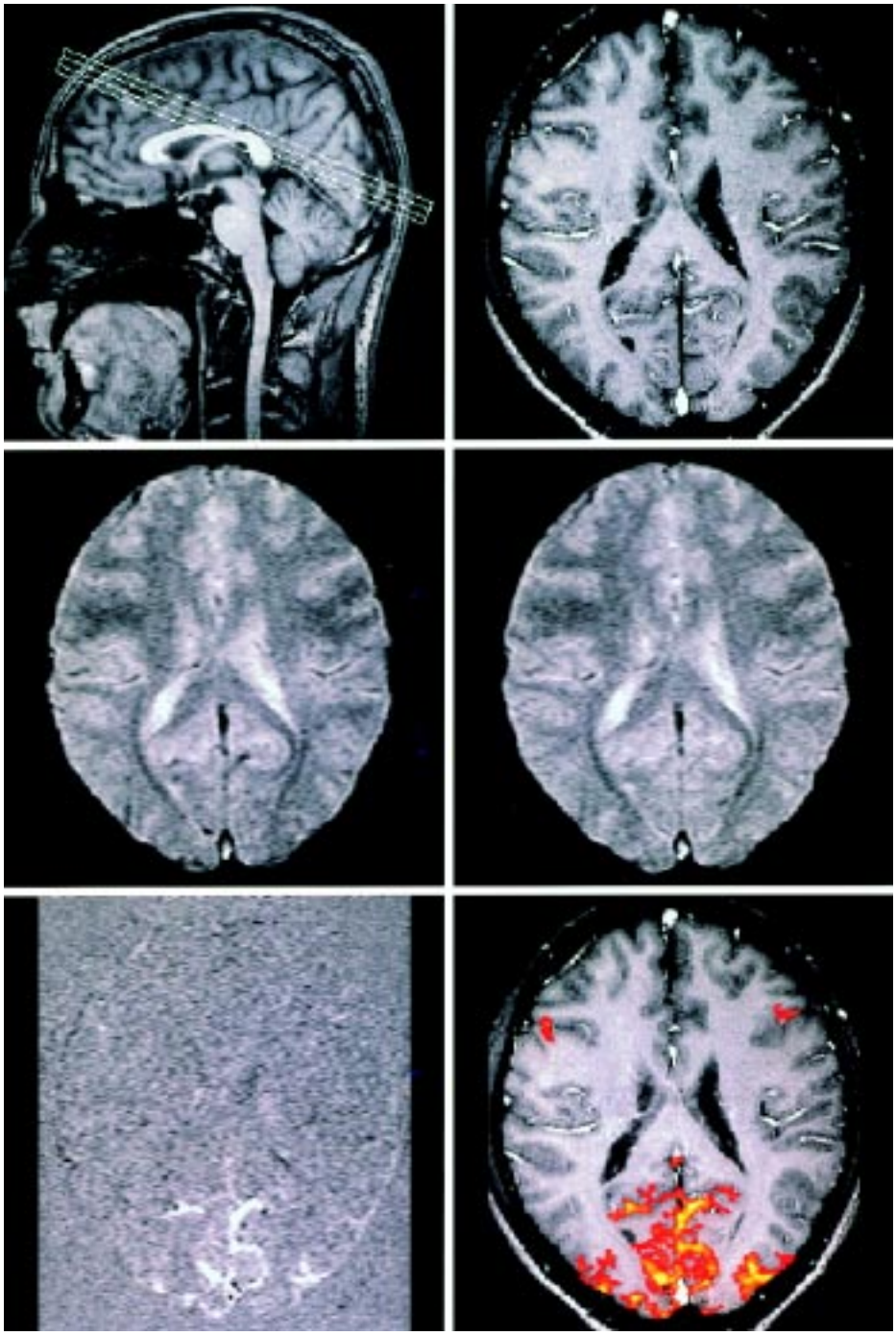

Fig. 5. Functional mapping of visual activation. (Top left) Definition of section orientation (2.0 T, 3D FLASH, TR/TE = 15/6 ms, flip angle 20°) and (top right) section anatomy and vasculature (FLASH, TR/TE = 70/6 ms, flip angle 50°). In going from darkness (middle left) to flickerlight stimulation (middle right), dynamic acquisitions of spin-density weighted images with T2* sensitivity (FLASH, 96 × 256 matrix, rectangular FOV 150 × 200 mm^2, slice thickness 4 mm, TR/TE = 62.5/30 ms, flip angle 10°, temporal rsolution 6 s) reveal a focal increase in MRI signal intensity, i.e., a decrease in deoxyhemoglobin, in visual cortex. (Bottom left) Difference map and (bottom right) color-coded activation map obtained by a pixel-by-pixel cross-correlation of signal intensity time courses with a reference function representing the stimulus protocol, compare Figure 6. (Modified from Kleinschmidt et al 1995a).

As shown in the bottom left part of Figure 5 the most simple approach is time-locked averaging of images representing the same functional state and subsequent subtraction, i.e., summation of images that are acquired during one condition (e.g., darkness) and subtraction of the result from that obtained for a different condition (e.g., flickerlight). The resulting difference map highlights cortical areas that are involved in processing flickerlight relative to darkness.

Correlation Map

A much more robust and also more sensitive approach than image subtraction stems from a correlation analysis. The technique exploits the temporal structure of the applied stimulation protocol and compares it to the oxygenation-sensitive MRI signal intensity time courses on a pixel-by-pixel basis (Bandettini et al 1993). Such strategies eliminate any statistical signal fluctuations as a source of contrast and are most helpful when recording multiple stimulation cycles that alternate between conditions. The bottom right part of Figure 5 depicts a map of correlation coefficients. Small activated areas of lower significance such as the frontal eye fields are more clearly distinguished than in the corresponding difference map.

Activity?

Whether the oxygenation-sensitive MRI responses reflect the enhanced firing or synchronization of neurons or indicate the recruitment of new though overlapping populations of specialized neurons within visual cortex cannot be decided from the MRI experiment. We need to keep in mind that even high-resolution studies in general are too coarse to resolve the columnar organization of the human cortex.

MRI Signal Intensity Time Courses

Figure 6 depicts selected time courses from regions-of-interest (ROI) in the primary visual cortex, the frontal eye field, and non-activated frontal gray matter for the experiment shown in Figure 5. The time courses reveal stimulus-induced responses to visual activation that tightly follow the sixfold application of a stimulation cycle comprising 18 s of flickerlight (shaded boxes) and 36 s of darkness.

The bottom trace in Figure 6 refers to a reference vector that mimics the temporal structure of the protocol shifted by one image (6 s) to account for hemodynamic latencies of the flow-induced change in blood oxygenation. This boxcar function was employed to calculate the color-coded map of correlation coefficients shown in the bottom right panel of Figure 5.

Calibration?

Mapping of brain activation relies on suitable physiologic models and mathematical methods that identify stimulus-related changes in MRI signal intensity time courses. Because the dynamic MRI signal may be characterized by its amplitudes, frequencies, and phases (relative to the applied paradigm), there are manifold ways of extracting functional information.

Although amplitude-based methods such as differences, variances, or statistical treatments (e.g., t or χ^2 tests) are possible, a reliable quantification and calibration of MRI signal strengths in terms of "oxygenation" or degree of "activity" is not possible. Attempts to calibrate T2* relaxation rates with respect to the arterial oxygen saturation are time-consuming and mainly performed in physiologically well-controlled animal experiments.

Mathematics

It is therefore well accepted to rely on relative amplitudes and to analyze the temporal evolution of signal changes. Pertinent techniques attempt to classify temporal properties by *correlation analyses* or equivalent frequencies by *Fourier analyses*. Further ap-

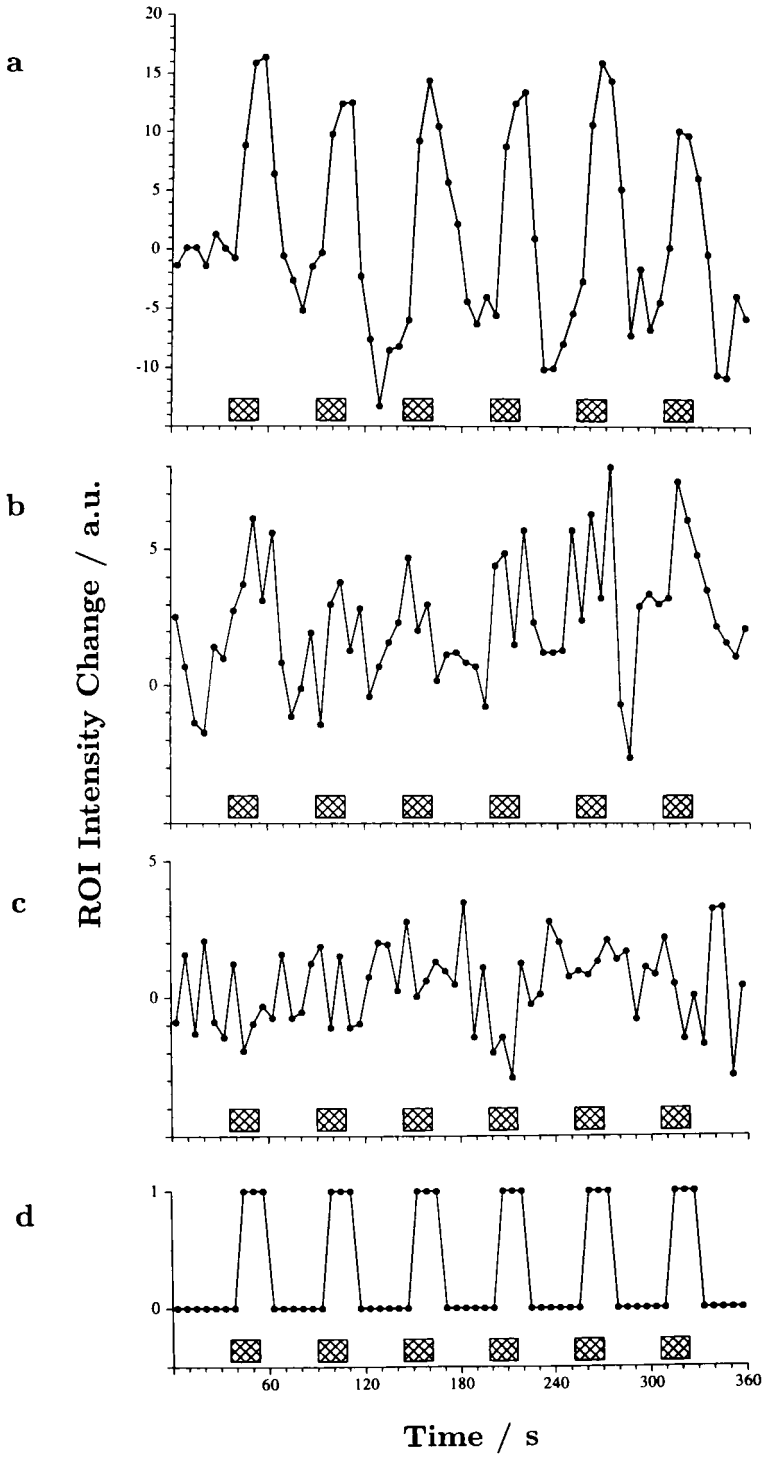

Fig. 6. Time courses of oxygenation-sensitive MRI signal intensities (2.0T, FLASH, TR/TE = 62.5/30ms, flip angle 10°, temporal resolution 6s) from regions-of-interest in (a) primary visual cortex, (b) frontal eye field, and (c) non-activated frontal gray matter (control) of a single subject in response to visual activation (18s of flickerlight vs. 36s of darkness). (d) Reference function that mimics the temporal structure of the stimulation protocol shifted by one image (6s) to account for hemodynamic latencies. This boxcar function was employed to calculate the thresholded map of correlation coefficients shown in Figure5.

proaches are *principal component analyses* and *fuzzy clustering algorithms*. However, neither is this list complete nor is a comprehensive description within the scope of this article.

Mathematical strategies for data analysis also need to take into account the noise characteristics of the experimental data. In optimized MRI systems the noise is of a physiologic rather than instrumental origin. Of course, the specifics also depend on the spatial integration (resolution) of vascular and/or tissue components and the temporal resolution relative to the hemodynamic responses and other modulatory effects such as breathing. Moreover, any post-acquisition data manipulation, the use of temporal and/or spatial filters or even artificial "baseline" or "drift" corrections may have strong influences on the resulting activation maps.

Statistical Maps and Beyond

Correlations

A preferred and robust method for data analysis is a cross-correlation of pixel intensity time courses with a reference function (Bandettini et al 1993). The method is robust against uncorrelated signal fluctuations, more sensitive to small or weakly activated areas than amplitude-based techniques, and flexible with regard to the applied paradigm and its temporal structure.

The choice of a reference function for cross-correlation may be a measured pixel intensity time course, a mathematical representation of the stimulation protocol, a real or hypothesis-driven model function, or even an EEG signal recorded in parallel to the MRI acquisition. The activation paradigm does not need to be periodic when taking the value of the cross-correlation function at zero time lag, i.e., the well-known correlation coefficient, which also results in fast calculations.

Histograms

An unprocessed map of correlation coefficients is a neutral representation of values between –1 (antiphase correlation), zero (no correlation), and +1 (perfect correlation) assigned to each pixel. To identify specific areas that are activated in association with an applied paradigm, pertinent maps need to be thresholded based on the statistical significance of the underlying MRI signal alterations.

Figure7 shows two histograms of correlation coefficients obtained for dynamic MRI acquisitions in the absence and presence of visual stimulation, respectively. Without activation the "noise" distribution of correlation coefficients is symmetric and centered at zero. Brain activation causes a deviation from the noise distribution at high positive (or negative) correlation coefficients.

Thresholds

Because differences in systemic hemodynamic responsiveness and motion stability cause intertrial variabilities that affect the center and width of the underlying noise distribution, it is not advisable to use absolute correlation coefficient thresholds for defining activation. Moreover, a single fixed threshold would result in a trade-off between specificity (e.g., by emphasizing only a few highly significantly activated foci at the expense of adequate area delineation) and sensitivity (e.g., by using a low threshold that allows for extended areas at the expense of including considerable noise).

Invariance against intertrial differences as well as adequate visualization of activated areas may be achieved by the following procedure (Kleinschmidt et al 1995a) schematically indicated in the right-hand part of Figure7.

Noise

A symmetrized noise distribution is reconstructed from the actual activation map by fitting the central part of the distribution to a symmetric function after identifying the center position and the full width at half maximum. This procedure allows rescaling of

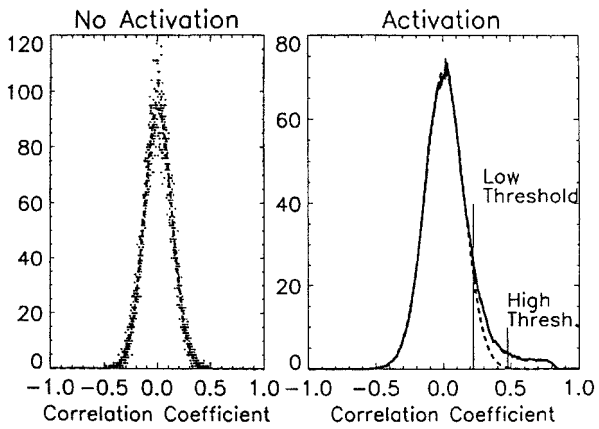

Fig. 7. Distribution of correlation coefficients for an experiment (left) without and (right) with visual activation using darkness as control state. In the right histogram the presence of activation is indicated by a deviation of the actual distribution (solid line) from the symmetrized noise floor (dashed line). The noise distribution is reconstructed from the central part of the actual distribution. The area between both distributions refers to the elevated number of pixels with high positive correlation coefficients.

correlation coefficients into percentile ranks with respect to the integral of the noise distribution. The percentile rank describes the probability of pixels at or above a given correlation coefficient to be noise, i.e., the error probability when assuming that such a pixel is "activated".

Specificity

While the procedure is still based on correlation coefficients, it generates robustness against variability of correlational noise. A high percentile rank (or correspondingly low error probability) is used as a threshold to define primary sites of activation. For the example shown in Figure 5 the activation map (bottom right) represents a thresholded map of correlation coefficients at the 99.99 % percentile for identifying significant activation with high specificity.

Sensitivity

The full spatial extent of an activated brain area may be mapped by adding directly neighboring pixels to highly significant foci provided their lower correlation coefficients are high enough to contribute to the deviation from the noise distribution. The rationale behind this is that inspection of correlation coefficient maps without any threshold reveals the activation foci to be embedded within clusters of elevated correlation coefficients. This tight topographic relationship as the "peak of the mountain" may be exploited to improve sensitivity without losing specificity: while identifying significant activation by a high threshold, adequate area delineation may be achieved by iteratively incorporating nearest neighbors that exceed a lower threshold derived from the difference between the actual and the noise distribution.

SPM etc.

Most research teams have developed their own analysis programs that may or may not be available on request. A popular, semi-automated, and more standardized program is SPM (Friston 1995). The package was originally developed for Statistical Parametric Mapping using low-resolution (static) PET images, but now contains tools suitable for the analysis of MRI data sets.

Regardless of which program is selected, both the methodologic novice and the cognitive neuroscientist who only wants to "use" the technique as a problem solver are strongly advised to follow a data-driven approach rather than to blindly rely on the performance of a black box evaluation program. In particular, it is recommended to frequently check the quality of the acquired raw images and to visualize unprocessed MRI signal intensity time courses.

Visualization

Once data acquisition and evaluation have led to an activation map, additional processing may be necessary to accomplish further scientific goals or clinical needs. In most cases pertinent tasks aim at a more advanced visualization of cross-sectional maps. They include image integration by matching brain function and co-registered individual 3D anatomy as well as surface rendering of combined data sets (e.g., for presurgical planning).

In neuroscience, transformation of individual activation maps into standardized brain atlases may serve the purpose of intersubject averaging to enhance sensitivity or to separate common and individualized cognitive strategies. In addition, the procedure allows for a comparison of the functional brain anatomy with complementary information on the cerebral microvasculature or cytoarchitecture. Standardized maps are also a prerequisite for the combination of data across modalities. Many of the aforementioned programs are still under development.

Physiologic Aspects of Brain Activation

Coupling

The critical link between a focal change in neuronal activity and MRI-detectable observables is the neurovascular coupling (e.g., see Villringer and Dirnagl 1995). It is therefore mandatory to control the influence of hemodynamic and metabolic parameters on the mapping process.

Hemoglobin

Provided that proper acquisition parameters are chosen, dynamic MRI of brain activation relies on BOLD contrast reflecting changes in the absolute concentration of deoxyhemoglobin. This understanding is not only supported by animal experiments but directly confirmed by simultaneous recordings using oxygenation-sensitive MRI and near-infrared optical spectroscopy of human motor activation (Kleinschmidt et al 1996).

This section introduces some of the mechanisms that determine the net cerebral blood oxygenation and putatively interfere with activation-induced responses to functional challenge.

Modulations of the Hemodynamic Response

Apart from the desired task-related adaptation in neuronal activity, modulations of the hemodynamically driven BOLD MRI contrast may arise from intrasubject and intersubject differences in other cognitive or emotional processes (e.g., attention and anxiety) or even systemic adjustments (e.g., heart rate and blood pressure). In addition, amplitude and temporal characteristics may be subject to changes in neurovascular responsiveness in relation to age (e.g., in early infancy and in the elder population), nutrition and medication (e.g., vasoactive and psychotropic drugs), or neuropathology (e.g., cerebrovascular disease). It is also likely that BOLD responses reveal a topographic dependence on brain systems as regional differences in neuroanatomy, microvasculature, and neurotransmitter systems are well established.

Neuroactive Drugs

Obvious examples of an interference with the cerebral blood oxygenation are direct pharmacologic interventions.

Figure 8 shows BOLD MRI responses to the administration of psychotropic drugs such as diazepam and metamphetamine. The effects of depression and stimulation of cerebral activity are significantly different for the two drugs applied. Relative to signal strength during injection, metamphetamine elicits a 1.0 % signal increase 3–4 min after the end of injection, whereas diazepam abolishes this effect.

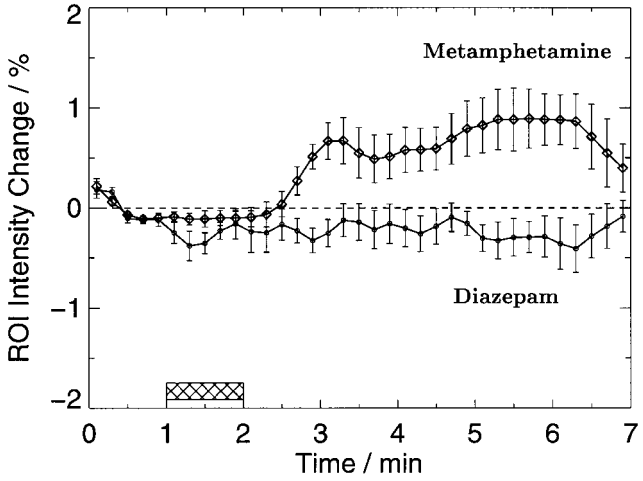

Fig. 8. Time courses of oxygenation-sensitive MRI signal intensities (2.0T, FLASH, TR/TE = 62.5/30ms, flip angle 10°, temporal resolution 12s) in response to pharmacologic stimulation and depression of cerebral activity by the intravenous administration (cross-hatched bar) of 15mg metamphetamine (upper curve) and 10mg diazepam (lower curve). The data originate from a whole brain section and represent a grand average across healthy young subjects ($n = 7$). Drug-specific responses are a signal increase after metamphetamine and a steady or mildly decreased signal intensity after diazepam, respectively. Vertical lines indicate the standard error of the mean. (Modified from Kleinschmidt et al 1999).

The metamphetamine-induced signal increase is more pronounced in subcortical gray matter structures and cerebellum than in frontotemporal cortical gray matter. These differences support the hypothesis that pertinent responses not only reflect global cerebral hemodynamic adjustments but also localized perfusion changes coupled to alterations in synaptic activity. The occurrence of a placebo response is best explained by expectancy and may provide a confounding factor in the design of functional activation experiments.

Vasoactive Drugs

The application of vasoactive drugs such as acetazolamide (vasodilation) and aminophylline (vasoconstriction) provides an even more direct interaction with cerebral blood flow and its effect on the deoxyhemoglobin concentration. Figure9 shows pertinent responses as well as their modulation of activation-induced signal changes in visual cortex.

Vasodilation

Administration of acetazolamide yields a generalized increase of the oxygenation-sensitive MRI signal in cortical (and subcortical) gray matter. As shown in the upper part of Figure9 the process starts about 1min after drug application and reaches a plateau phase after 5–10min. Assuming unchanged oxidative metabolism, it reflects a venous hyperoxygenation, i.e. decreased deoxyhemoglobin, due to elevated cerebral perfusion. This is a consequence of hypercapnia caused by inhibition of carbonic anhydrase.

The marked reduction of activation-induced MRI signal changes after vasodilation indicates an attenuation of vasomotor activity. Taking intersubject variability into account, the data reveal an individually modulated autoregulatory responsiveness to functional challenge. In cases of a truly "exhausted" reserve capacity, autoregulation may fail to generate any MRI signal change which effectively eliminates the detectability of brain activation at the physiologic level.

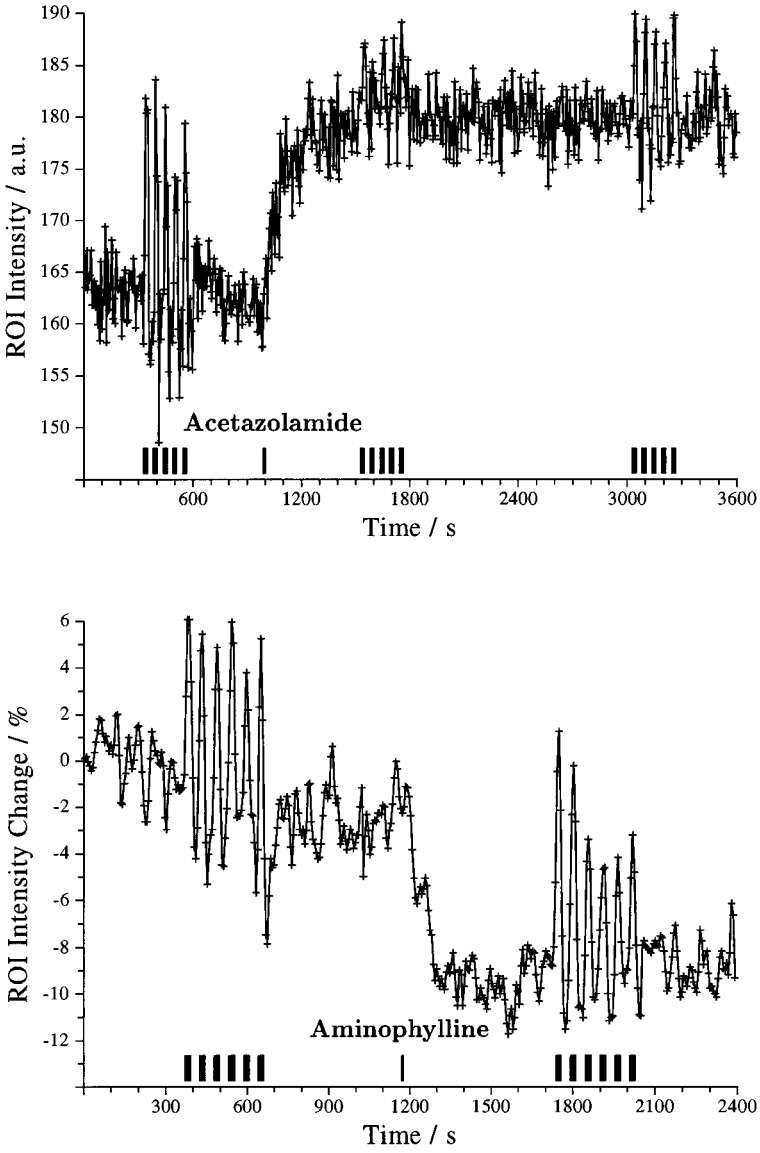

Fig. 9. Time courses of oxygenation-sensitive MRI signal intensities (2.0T, FLASH, TR/TE = 62.5/30ms, flip angle 10°, temporal resolution 6s) in response to visual activation (5 cycles, 18s flickerlight vs. 36s of darkness, solid bars) before and after the intravenous administration of 1.0g acetazolamide (top) and 0.2g aminophylline (bottom). The data originate from a region-of-interest in the visual cortex of two different subjects consecutively imaged over a period of 60min (top) and 40min (bottom), respectively. Whereas vasodilation results in MRI signal increases (i.e., decreased deoxyhemoglobin) and significant attenuation of functional responses, vasoconstriction yields a corresponding signal decrease (i.e., increased deoxyhemoglobin) but no change of the response strength to visual activation. (Modified from Bruhn et al 1994 and Kleinschmidt et al 1995b).

Vasoconstriction

The administration of aminophylline results in a fast decrease of the MRI signal intensity as shown in the lower part of Figure 9. The respective increase of deoxyhemoglobin may be explained by the combination of reduced blood flow and unchanged or even slightly enhanced oxygen consumption as aminophylline includes a neural excitatory action in addition to its vasoactivity. The fact that the post-injection response strength

to visual activation is neither diminished nor enhanced suggests the involvement of different mediator systems for hemodynamic adjustments of pharmacologic and functional challenges, respectively.

Pathology

Special care is required when applying physiologic mapping of neuronal activation to patients. Apart from direct effects of space-occupying lesions, neurodegenerative and neurometabolic disorders may have consequences affecting cerebral autoregulation or other aspects of the neurovascular (neurometabolic) coupling. Cerebrovascular disease that leads to hemodynamic compromise has already been demonstrated to completely disrupt the expected MRI response in individual patients. Further examples are patients receiving medication either related or unrelated to their neurologic problem (e.g., psychiatric patients in the elder population) or studies under anesthesia. In the latter case the affected regulation of cerebral blood flow most likely precludes any meaningful applications.

Response Functions and Protocol Timings

There is still limited knowledge about the temporal evolution and interplay of activation-induced adjustments of cerebral blood flow, blood volume, and oxidative metabolism in humans and its effect on the "functional contrast". In general, the development of the real-time BOLD MRI signal will be the result of multiple regulative processes with different time constants. Such contributions may critically affect the interpretation of MRI responses, in particular when these are acquired with use of repetitive stimulation protocols.

The question arises whether focal changes in neuronal activity result in a characteristic physiologic MRI response function. Figure 10 demonstrates typical signal patterns for visual activation protocols ranging from sustained stimulation to the presentation of single brief stimuli. The most important finding from these studies is the identification of a slow physiologic process that complements the initial signal rise after stimulation onset.

Fast Process

The fast positive BOLD response is usually ascribed to a hyperoxygenation caused by a rapidly increased blood flow (i.e., oxygen delivery) that is not matched by an immediately effective upregulation of oxidative metabolism (i.e., oxygen consumption).

Slow Process

In contrast, the slow signal changes refer to an attenuation of the hemodynamic response curve during ongoing stimulation (i.e., a relative deoxygenation) and the recovery of a pronounced signal undershoot after the end of stimulation to pre-stimulation baseline, e.g., seen for sustained activation in panel A of Figure 10.

Whereas checkerboard responses remain almost unaffected during ongoing activation (less than 20 % signal attenuation), all other stimuli including flashing diffuse light and real movies result in more than a 50 % decrease of the initial signal response after 6 min of stimulation. Potential factors that might explain this discrepancy include stimulus-dependent regulations of blood flow, blood volume, and oxygen consumption or differential degrees of habituation and adaptation.

Mechanisms

The most likely candidates for the slow process are adjustments of oxidative glucose consumption (Frahm et al 1996) and a modulation of the venous blood volume (Buxton et al 1998). These mechanisms may require a certain delay to become quantitatively detectable against the dominating flow-related MRI signal changes both after the onset

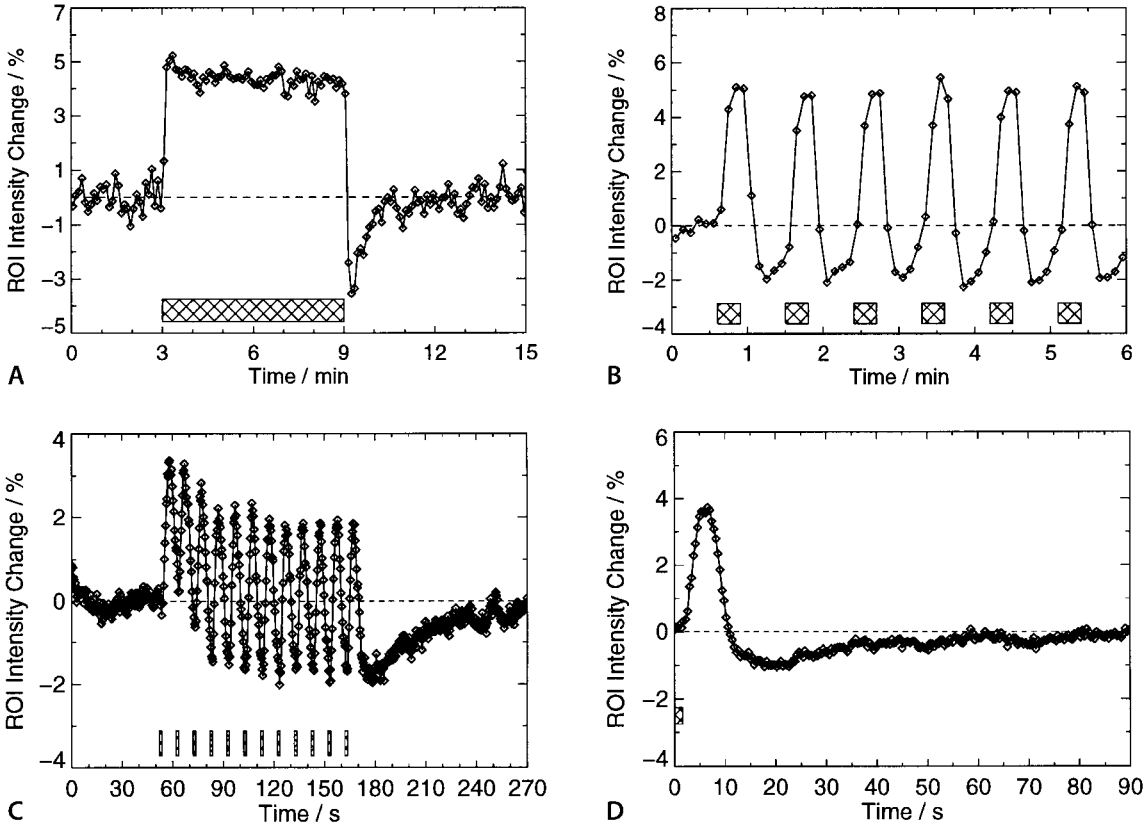

Fig. 10. Time courses of oxygenation-sensitive MRI signal intensities (2.0 T) for various protocols of visual activation (checkerboard vs. darkness, cross-hatched bars). (a) Responses to sustained activation ($n = 7$) for a period of 6 min and (b) to repetitive activation ($n = 7$) by a 18 s/36 s protocol (FLASH, TR/TE = 62.5/30 ms, flip angle 10°, temporal resolution 6 s). (c) Responses to repetitive activation (n=8) by a 1.6 s/8.4 s protocol and (d) to single events (n=5) by a 1.6 s/90 s protocol (EPI, TR/TE = 400/54 ms, flip angle 30°, temporal resolution 0.4 s). The curves represent mean values of all pixels with statistically significant stimulus-related signal alterations averaged across subjects. (Modified from Krüger et al 1998 and Fransson et al 1998a).

and end of stimulation. However, independent of the underlying mechanism, the existence of two processes with different time constants is directly relevant for mapping studies that are commonly based on short protocol timings.

Repetitions

The time courses for repetitive visual activation in panels B and C of Figure 10 represent 6 cycles of a 18 s/36 s protocol and 12 cycles of a 1.6 s/8.4 s protocol. Both studies reveal a "baseline drift" during cyclic stimulation that reaches a new steady state after about 2 min. This observation is in close agreement with the presence of a slow physiologic process and seems to represent the accumulation of undershoot contributions from preceding stimuli. The end of repetitive stimulation is characterized by a marked undershoot with an amplitude of up to –2 % below pre-stimulation baseline and a duration of 60–90 s.

The relative peak-to-peak signal difference or "functional contrast" between successive stimuli remains almost unchanged throughout the experiments at about 7 % for the 18 s stimulus and 4 % for the 1.6 s stimulus, respectively.

Single Trials

The qualitative agreement of responses for different stimulus durations motivated studies of single events as shown in panel D of Figure 10. A close inspection of the response

profiles obtained for brief visual stimuli with long interstimulus intervals reveals a 1.5–2.0 s hemodynamic latency, a positive 4 % signal increase at 5–7 s after stimulus onset, and a signal undershoot of about –1 % at 15–20 s after stimulus onset. Return to pre-stimulation baseline is accomplished 60–90 s after the end of the stimulus. It indicates that rather long periods are required if activation-induced BOLD MRI signal alterations need to be physiologically 'decoupled' from each other.

Conversely, shorter interstimulus periods physiologically 'couple' repetitive stimuli in such a way that their BOLD MRI responses become contaminated by the pre-stimulation history.

Similar findings hold true for subsecond visual stimuli as well as for paradigms replacing darkness as the only control state.

Noise

Response functions such as in panel D of Figure 10 create an important link between brief cortical events and much slower physiologic fluctuations that modulate the dynamic BOLD MRI signal even in the absence of functional challenge. Excluding instrumental noise, an analysis of such low frequency "noise" in the primary sensorimotor and visual system has already been used to generate maps of functional connectivity (Biswal et al 1995).

Initial Dip

Data from near-infrared optical imaging of exposed visual cortex in animals have suggested a rise of deoxyhemoglobin within the first 2 s of activation due to an immediate increase in oxygen consumption at the site of neuronal activation. However, it is not entirely clear to which degree optical data from animals may be extrapolated to MRI studies of humans. For example, both methodologies focus on different tissue elements: whereas MRI detects intravoxel susceptibility changes from all vascular components that contribute to one image voxel, optical experiments commonly exclude all signals from vessels that are identifiable by visual inspection.

In this context, it should be emphasized that time-locked averaging of multiple activation cycles from repetitive protocols with insufficient recovery periods (e.g., traces B and C of Figure 10) may give rise to an artifactual "initial dip". The effect is caused by a "wrap around" of real-time signal contributions and particularly applies to the undershoot of preceding activations which folds back into the "silent" latency phase of a subsequent activation cycle. When ensuring complete decoupling of successive stimuli by using long interstimulus recovery periods (e.g., in trace D of Figure 10), the wrap around effect and the resulting dip vanish.

Event-Related Recordings

Rather than only reducing the stimulus duration, mapping protocols may be optimized by decreasing the interstimulus periods. Pertinent protocols attempt to identify individual "events" in a stream of rapidly presented stimuli and should facilitate the MRI adaptation of paradigms commonly applied in cognitive neuropsychology.

Figure 11 demonstrates real-time BOLD MRI responses to a series of 1 s visual stimuli when the interstimulus interval is reduced from 89 s to 6 s and 3 s, respectively.

Contrast

A key observation is a gradual decrease of the peak-to-peak difference between stimulus-related positive and negative signal deflections. The effect becomes dramatic for interstimulus durations of less than about 5–6 s which corresponds to the time-to-maximum response for brief visual stimuli.

The attenuation of the functional contrast reflects the insufficient time for the development of both the full positive BOLD MRI response and its effective reversal after the end

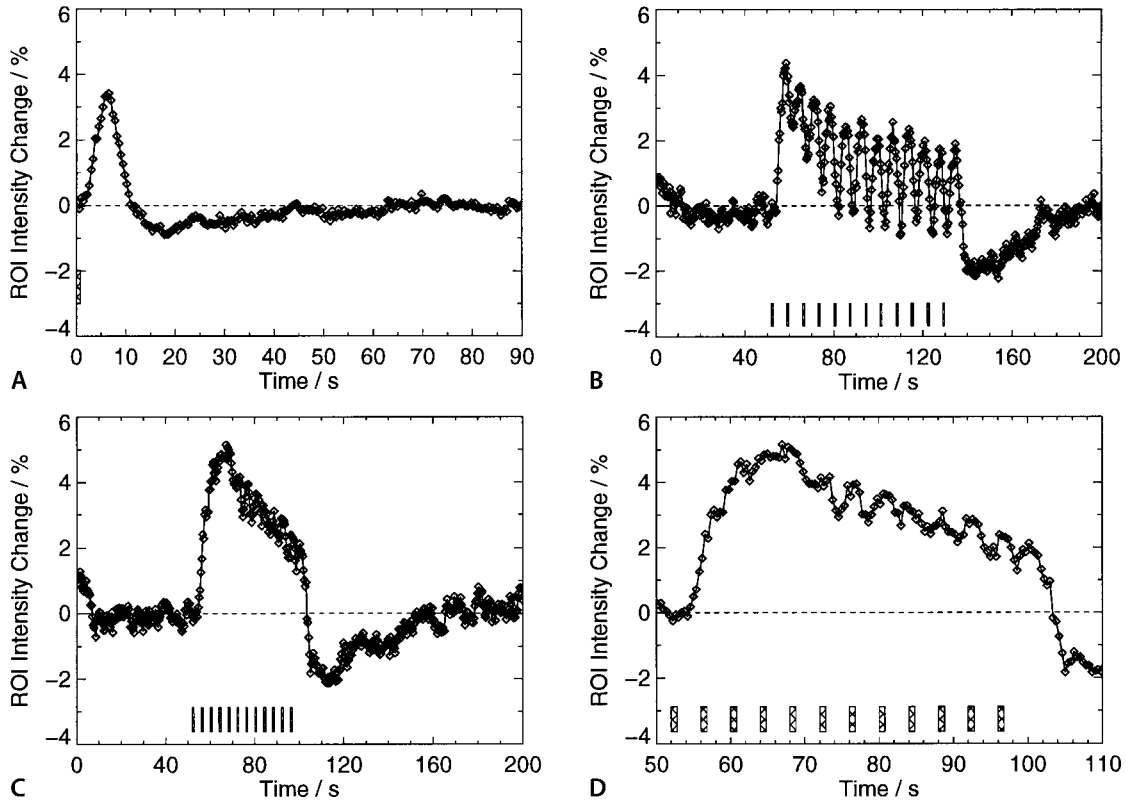

Fig. 11. Time courses of oxygenation-sensitive MRI signal intensities (2.0 T, EPI, TR/TE = 400/54 ms, flip angle 30°, temporal resolution 0.4 s) for protocols comprising a 1 s period of visual activation (checkerboard vs. darkness, cross-hatched bar) but different interstimulus periods. The real-time responses refer to (a) a 1 s/89 s, (b) a 1 s/6 s, and (c) a 1 s/3 s protocol. (d) Enlarged view of the responses shown in (c). The curves represent mean values of all pixels with statistically significant signal alterations averaged across subjects (n=6) and stimulation cycles. (Modified from Fransson et al 1998b).

of the stimulus. The cumulative effect from several undershoots leads to a new equilibrium with an apparent "baseline" well below the pre-stimulation baseline and a pronounced undershoot after the end of the last stimulation cycle. It also affects the individual real-time MRI responses in such a way that the almost nonexistent functional contrast during the initial phase of the event-related paradigm enhances during the first 4 (Figure 11B) or 6 cycles (Figure 11C,D) for interstimulus intervals of 6 s and 3 s, respectively.

Mapping

The activation maps shown in Figure 12 reveal adequate spatial congruence of activated brain regions for the 1 s/89 s, 1 s/6 s, and 1 s/3 s protocols. They are obtained by cross-correlation of pertinent time courses with suitable reference functions mimicking the protocol timings as well as hemodynamic latencies, rise and fall times.

Notwithstanding ongoing discussions about a linear or nonlinear system analysis of responses elicited by event-related paradigms, the results confirm the ability to map condition-specific populations of neurons as long as dynamic MRI data sets provide sufficient functional contrast at the physiologic level. More specifically, this finding only applies to processing of identical stimuli in the visual cortex and under conditions where the individual responses can be separated in time.

Deactivation

In general, complex paradigms may pose further complications because they tend to involve activity switches between arbitrary conditions that may yield both MRI signal in-

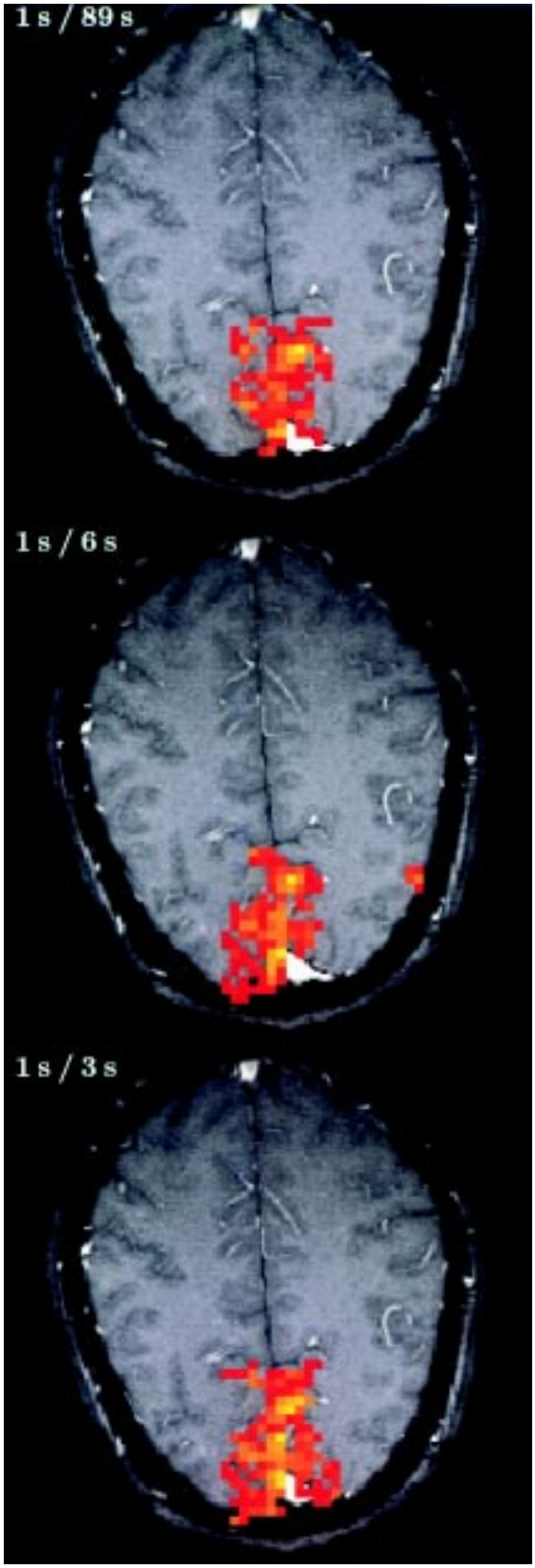

Fig. 12. Spatial congruence of visual cortical areas of a single subject activated by (top) a 1 s/89 s, (middle) a 1 s/6 s, and (bottom) a 1 s/3 s protocol using the same paradigm as in Figure 10. The maps are superimposed onto a reference image (rf-spoiled FLASH, TR/TE = 70/6 ms, flip angle 60°) delineating anatomy and macrovasculature. (Modified from Fransson et al 1998b).

creases and decreases. Future work will need to address "deactivation" at the physiologic level and develop evaluation strategies to analyze bidirectional switches between states of variable degrees of neuronal activity.

Paradigm Design

A most promising feature of MR functional neuroimaging is the flexibility in the design of experimental paradigms. A preliminary list of possibilities includes
- block structures comparing two functional states,
- multiplexed or interleaved block structures with multiple states,
- event-related paradigms,
- triggered acquisitions, and
- noise analyses without a functional challenge.

Some Basic Structures

Blocks

So far, many functional MRI examinations employ a design based on a block structure A vs. B. The paradigm compares the neuronal representations of two distinct conditions – often under the simplified assumption of an activated state A (e.g., motor activity, visual stimulation) and a control condition B (e.g., motor rest, darkness).

Even the simple block structure requires further consideration. For example, the statistical power of the data analysis depends on the number of images acquired per condition as well as on the number of repetitions (or activation cycles). In addition, the choice of a temporally symmetric or asymmetric presentation of A and B conditions as well as their absolute durations may influence the task performance, the data analysis, and the resulting map. An important aspect may be the order or direction of comparisons: if A vs. B corresponds to activation processes, B vs. A will indicate deactivation processes in either overlapping or different regions even when the data is taken from the same experiment.

Multiplexing

Without the doubtful assumption of a "resting" brain, more reasonable concepts adopt the view of qualitatively equivalent states of activity that only quantitatively differ in the degree of neuronal firing or synchronization or the extent of neuronal subpopulations involved. These ideas lead to the development of multiplexed or interleaved paradigm structures, where multiple conditions may be compared to each other or suitable combinations. A simple example demonstrating marked differences in the underlying question as well as in the results stems from the replacement of a task vs. control structure by a task 1 vs. task 2 design in a study of finger somatotopy in the human motor hand area (see below).

Multiplexed designs offer better chances to optimize cognitive paradigms with respect to maintaining attention and avoiding habituation and expectancy. They are also efficient in allowing for multiple differential comparisons within a single experimental run. In practice, the use of physiologically optimized durations of 8–10 s per condition as well as of statistically recommended 4–6 repetitions limits the number of different states to about 10 as measurement times should be kept to below 10 min with regard to subject compliance and motion problems.

A special variant are serial or incremental variations of stimulus features such as eccentricity or angle of the visual field or frequency of an acoustic tone. Suitable analysis strategies provide direct access to the retinotopic or tonotopic organization of primary visual and auditory cortices, respectively.

Events

Event-related paradigms minimize the durations of stimulus presentations and interstimulus intervals in a multiplexed block paradigm and attempt to unravel the transient responses to and spatial representations of differential cortical events. A typical example is the "odd-ball" paradigm which tests the brain's capacity for identifying individual responses to novel events in a rapid stream of otherwise identical stimuli.

Nevertheless, the ability to separately analyze neuronal activity changes at the physiologic level depends on the ability to distinguish pertinent responses in time or space.

In general, we have to face activations in brain regions showing multi-functional encoding, i.e., overlap of subpopulations of neurons with different functional representations. Such observations already apply to visual and sensorimotor areas (see below), but are even more likely to occur for higher order cognitive processing. Accordingly, in order to distinguish responses with similar spatial encodings, we need to retain a sufficient "decoupling" of physiologic responses in time and thereby ensure residual functional contrast for spatial mapping.

It has also been proposed to temporally randomize stimulus presentations in event-related paradigms to alleviate the degradation of the functional contrast for short interstimulus periods.

EEG

Another class of experiments are dynamic MRI acquisitions where the data analysis is performed in accordance with an (externally) recorded "trigger" signal. Although still hampered by technical difficulties, a prominent application is the correlation of oxygenation-sensitive MRI signal changes with specific patterns in the EEG. For example, it is conceivable to detect and map the physiologic correlates of epileptic activity in the interictal state.

Other possibilities are correlations with the application of repetitive transcranial magnetic stimulation (e.g., in treating depression) or involve the recording of psychophysical or behavioral parameters.

Selected Applications

Foreseeable clinical applications range from contributions to presurgical planning (e.g., sensorimotor activity, hemispheric language dominance) to mapping of disease-related dysfunction (e.g., blindsight) and cortical (re-) organization. The latter refers to both short-term plasticity (e.g., learning, memory) and long-term changes during early brain development or rehabilitation and recovery after brain injury. Still rather premature applications aim at the functional mapping of cognitive and emotional deficits of psychiatric patients.

Somatotopy

A simple though illustrative example of the importance of a proper paradigm is the analysis of finger somatotopy in the human motor cortex. Fine-scale somatotopic encoding in brain areas devoted to sensorimotor processing may be questioned when using a design of self-paced isolated finger movements vs. motor rest. Pertinent experiments result in extensive overlap of spatial representations covering the entire hand area for almost all fingers. The design asks for all locations of finger representations and addresses somototopy only in the sense of true functional (spatial) segregation.

In contrast, Figure 13 demonstrates markedly different results when the paradigm directly switches between individual finger movements. This design asks for cortical response preference or "qualitative" somototopy rather than for mere neuronal activity. Using functional maps at high spatial resolution, the comparative paradigm reveals foci of differential activation which display an orderly medio-lateral progression in accordance with the classical cortical motor homunculus.

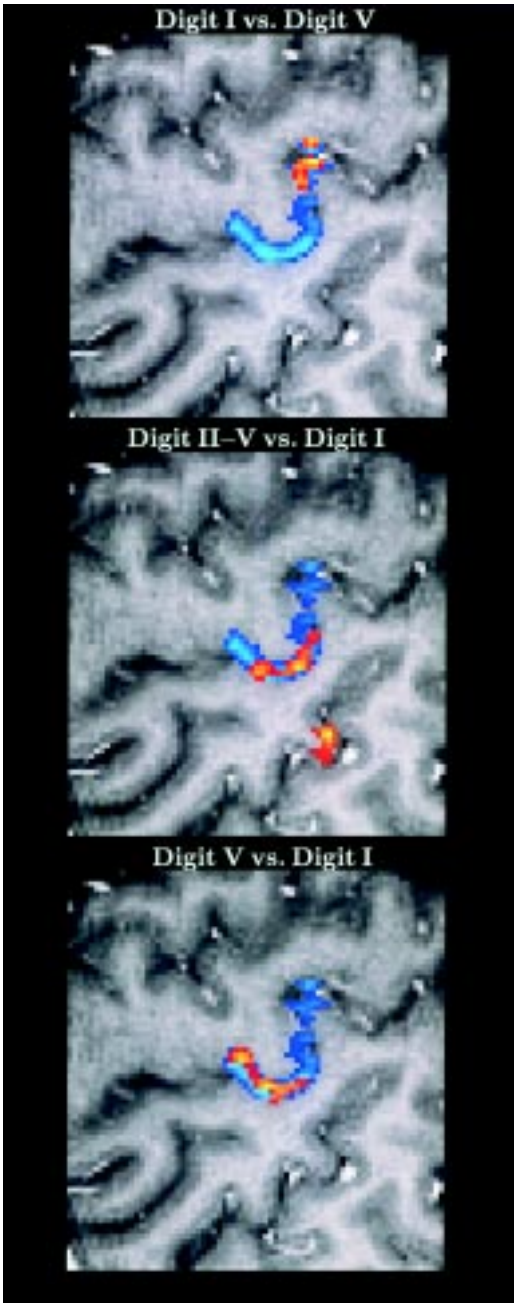

Fig. 13. Functional predominance of cortical representations of individual finger movements of the right hand (coded in red) in the left-hemispheric primary motor hand area (coded in blue) of a right-handed subject. The hand area was delineated by a sequential finger-to-thumb opposition task of the right hand vs. motor rest. Finger movements were studied by a comparative paradigm design based on 6 cycles of a 18 s/36 s protocol. Despite overlap of representations, functional predominance of (top) the thumb vs. little finger, (middle) index through little finger vs. thumb, and (bottom) little finger vs. thumb follows a somatotopic arrangement in covering the lateral, intermediate, and medial portion of the hand area, respectively (2.0 T, FLASH, TR/TE = 62.5/30 ms, flip angle 10°, measuring time 6 s, spatial resolution 0.78 × 1.56 mm^2 interpolated to 0.78 × 0.78 mm^2 during image reconstruction, section thickness 4 mm). (Modified from Kleinschmidt et al 1997).

From these design-specific findings it may be concluded that somatotopy within the hand area of primary motor cortex does not present as qualitative functional segregation but as quantitative predominance of certain digit representations embedded within a physiologically synergetic and anatomically interconnected joint hand area.

Language

Another example of paradigm-specific responses deals with the identification of an early visual area involved in language comprehension. Exploiting the MRI potential for testing a large number of differential paradigms within single sessions, the mapping process itself identified the relevant properties for separating “reading” from “seeing”.

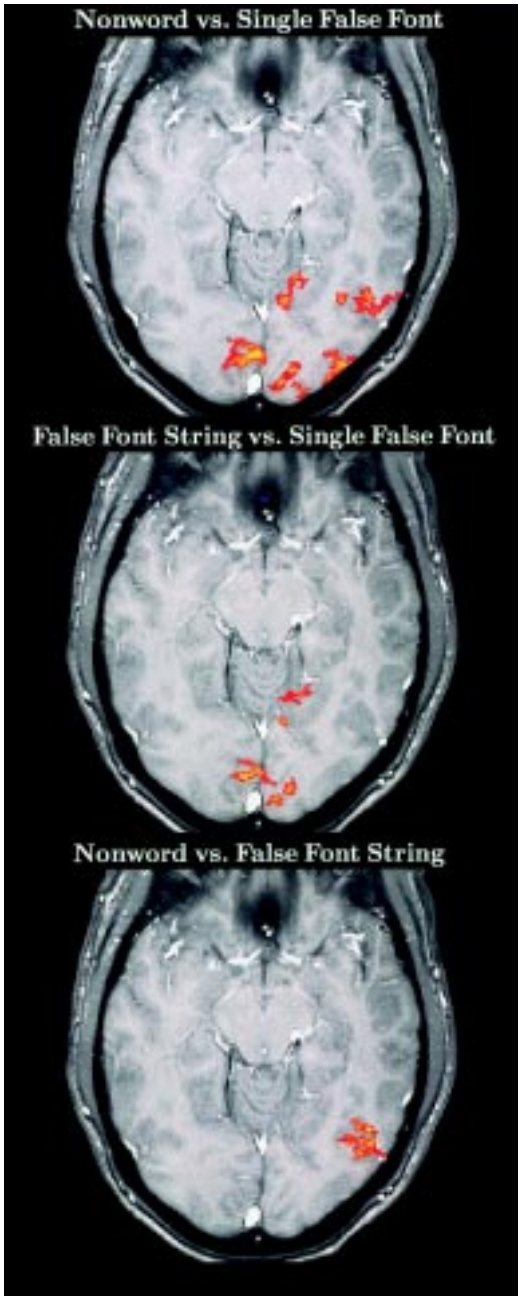

Fig. 14. Identification of an early visual area involved in language comprehension. (Top) Activations in ventral occipital cortex representative of a "global" paradigm comparing a nonword and a single false font with no lexical meaning. (Middle) Activations representative of horizontal length encoding ("seeing") obtained by comparing a string of false fonts vs. a single false font. (Bottom) Lateralized activations in a left-hemispheric region representative of processing lexical input ("reading") obtained by comparing a nonword vs. a length-matched string of false fonts. Experimental parameters were as in Figure 13. (In collaboration with Peter Indefrey and Colin Brown).

The top map in Figure 14 depicts responses in the ventral stream of the occipital (visual) cortex that are representative for viewing a pronounceable though meaningless "nonword" (e.g., debam) vs. a single false font with a complexity similar to that of a letter but no lexical character. Although the observed hemispheric lateralization suggests specific contributions representative for processing lexical input, the distributed areas may be further split into subcomponents by using paradigms with even more subtle cognitive differences than the leading experiment.

The middle part of Figure 14 indicates that the medial components in this subject correspond to simple length encoding along the horizontal median unraveled by a direct comparison of a string of false fonts vs. a single false font. Complementarily, the strictly

lateralized left-hemispheric region in the bottom map is indeed suggestive of early visual processing of lexical input as the used paradigm compared presentations of a nonword vs. a length-matched string of false fonts.

Acknowledgement: We are indebted to a large number of colleagues and co-workers including Harald Bruhn, Wolfgang Hänicke, Andreas Kleinschmidt, and Klaus-Dietmar Merboldt for invaluable contributions over the past 5 years.

References

Bachelard HS (1997) Magnetic resonance spectroscopy and imaging in neurochemistry. In: Agranoff B, Suzuki K (eds) Advances in neurochemistry, Vol 8. Plenum, New York

Bandettini PA, Wong EC, Hinks RS, Tikofsky RS, Hyde JS (1992) Time course EPI of human brain function during task activation. Magn Reson Med 25:390–397

Bandettini PA, Jesmanowicz A, Wong EC, Hyde JS (1993) Processing strategies for time-course data sets in functional MRI of the human brain. Magn Reson Med 30:161–173

Biswal B, Yetkin FZ, Haughton VM, Hyde JS (1995) Functional connectivity in the motor cortex of resting human brain using echo-planar MRI. Magn Reson Med 34:537–541

Blamire AM, Ogawa S, Ugurbil K, Rothman D, McCarthy G, Ellermann JM, Hyder F, Rattner Z, Shulman RG (1992) Dynamic mapping of the human visual cortex by high-speed magnetic resonance imaging. Proc Natl Acad Sci USA 89:11069–11073

Bruhn H, Kleinschmidt A, Boecker H, Merboldt KD, Hänicke W, Frahm J (1994) The effect of acetazolamide on regional cerebral blood oxygenation at rest and under stimulation as assessed by MRI. J Cereb Blood Flow Metab 14:742–748

Buxton RB, Wong EC, Frank LR (1998) Dynamics of blood flow and oxygenation changes during brain activation: The balloon model. Magn Reson Med 39:855–864

Fox PT, Raichle ME (1986) Focal physiological uncoupling of blood flow and oxidative metabolism during somatosensory stimulation in human subjects. Proc Natl Acad Sci USA 83:1140–1144

Frahm J, Bruhn H, Merboldt KD, Hänicke W (1992) Dynamic MRI of human brain oxygenation during rest and photic stimulation. J Magn Reson Imaging 2:501–505

Frahm J, Krüger G, Merboldt KD, Kleinschmidt A (1996) Dynamic uncoupling and recoupling of perfusion and oxidative metabolism during focal brain activation in man, Magn Reson Med 35:143–148

Fransson P, Krüger G, Merboldt KD, Frahm J (1998a) Temporal characteristics of oxygenation-sensitive MRI responses to visual activation in humans. Magn Reson Med 39:912–919

Fransson P, Krüger G, Merboldt KD, Frahm J (1998b) Physiologic aspects of event related paradigms in magnetic resonance functional neuroimaging. NeuroReport 9:2001–2005

Friston KJ, Holmes AP, Worsley KP, Poline JB, Frith CD, Frackowiak RSJ (1995) Statistical parametric maps in functional imaging: a general linear approach. Hum Brain Map 2:189–210 [http://www.fil.ion.ucl.ac.uk/spm]

Kleinschmidt A, Requardt M, Merboldt KD, Frahm J (1995a) On the use of temporal correlation coefficients for magnetic resonance mapping of functional brain activation. Individualized thresholds and spatial response delineation. Intern J Imag Sys Technol 6:238–244

Kleinschmidt A, Bruhn H, Steinmetz H, Frahm J (1995b) Pharmacologic manipulation of vasomotor tone studied by magnetic resonance imaging of cerebral blood oxygenation. J Cerebr Blood Flow Metab 15:S527

Kleinschmidt A, Obrig H, Requardt M, Merboldt KD, Dirnagl U, Villringer A, Frahm J (1996) Simultaneous recording of cerebral blood oxygenation changes during human brain activation by magnetic resonance imaging and near-infrared spectroscopy. J Cereb Blood Flow Metab 16:817–826

Kleinschmidt A, Nitschke MF, Frahm J (1997) Somatotopy in the human motor cortex hand area. A high-resolution functional MRI study. Eur J Neurosci 9:2178–2186

Kleinschmidt A, Bruhn H, Krüger G, Merboldt KD, Stoppe G, Frahm J (1999) Effects of sedation, stimulation, and placebo on cerebral blood oxygenation. A magnetic resonance neuroimaging study of psychotropic drug action. NMR Biomed in press

Krüger G, Kleinschmidt A, Frahm J (1996) Dynamic MRI of cerebral blood oxygenation and flow during sustained activation of human visual cortex. Magn Reson Med 35:797–800

Krüger G, Kleinschmidt A, Frahm J (1998) Stimulus dependence of oxygenation-sensitive MRI responses to sustained visual activation. NMR Biomed 11:75–79

Kwong KK, Belliveau JW, Chesler DA, Goldberg IE, Weisskoff RM, Poncelet BP, Kennedy DN, Hoppel BE, Cohen MS, Turner R, Cheng HM, Brady TJ, Rosen BR (1992) Dynamic magnetic resonance imaging of human brain activity during primary sensory stimulation. Proc Natl Acad Sci USA 89:5675–5679

Ogawa S, Lee TM, Kay AR, Tank DW (1990) Brain magnetic resonance imaging with contrast dependent on blood oxygenation. Proc Natl Acad Sci USA 87:9868–9872

Ogawa S, Tank DW, Menon R, Ellermann JM, Kim SG, Merkle H, Ugurbil K (1992) Intrinsic signal changes accompanying sensory stimulation: functional brain mapping with magnetic resonance imaging. Proc Natl Acad Sci USA 89:5951–5955

Stark DD, Bradley WG (1998) Magnetic Resonance Imaging, 3rd Edition. Mosby, St Louis

Turner R, Le Bihan D, Moonen CTW, DesPres D, Frank J (1991) Echo-planar time course MRI of cat brain oxygenation changes. Magn Reson Med 22:159–166

Villringer A, Dirnagl U (1995) Coupling of brain activity and cerebral blood flow: Basis of functional neuroimaging. Cerebrovasc Brain Metab Rev 7:240–276